

Elliptic flow of thermal photons and dileptons

U. Heinz^{a,1}, R. Chatterjee^b, E. Frodermann^a,
C. Gale^c, and D. K. Srivastava^b

^a*Department of Physics, The Ohio State University, Columbus, OH 43210, USA*

^b*Variable Energy Cyclotron Centre, 1/AF Bidhan Nagar, Kolkata 700 064, India*

^c*Department of Physics, McGill University, Montreal, Québec H3A 2T8, Canada*

Abstract

In this talk we describe the recently discovered rich phenomenology of elliptic flow of electromagnetic probes of the hot matter created in relativistic heavy-ion collisions. Using a hydrodynamic model for the space-time dynamics of the collision fireball created in Au+Au collisions at RHIC, we compute the transverse momentum spectra and elliptic flow of thermal photons and dileptons. These observables are shown to provide differential windows into various stages of the fireball expansion.

1 Introduction

The strong radial and elliptic flow of hadrons observed in relativistic heavy-ion collisions at RHIC have led to the important conclusion that the quark-gluon plasma (QGP) created in these collisions acts like a strongly coupled plasma with almost perfect liquid behaviour. This conclusion is based on the successful prediction of the hadron momentum distributions, in particular of their anisotropies in non-central collisions, by dynamical calculations which treat the expanding QGP as an ideal fluid. While no other equally successful model exists, one has to remain conscious of the fact that the new “perfect liquidity” paradigm is based on a model back-extrapolation of the measured data to the early stages of the collision which are not directly accessible with hadronic observables. There are strong arguments that this back-extrapolation is fairly unique [1] and hence that the above-mentioned qualitative conclusion is robust. On a quantitative level, however, the extraction from experimental data of the (small) QGP viscosity is presently hampered not only by the unavailability of consistent hydrodynamic codes for viscous relativistic fluids, but even more by uncertainties about the hydrodynamic effects of changes in the equation of state of the QGP matter [2] and about details of the initial conditions at the beginning of the hydrodynamic expansion stage [3,4].

* Work supported by the U.S. Department of Energy (U.H.), by NSERC of Canada and by the Fonds Québécois de Recherche sur la Nature et les Technologies (C.G).

¹ Invited speaker and corresponding author. *Email: heinz@mps.ohio-state.edu*

It would therefore be invaluable to have data on additional experimental observables which probe directly the earlier expansion stages and help to further constrain the space-time and momentum-space characteristics of the fireball expansion and the related model uncertainties. Electromagnetic probes, in particular direct photons and dileptons, provide such observables. Due to the weakness of the electromagnetic interaction, real and virtual photons are not created abundantly, making their measurement difficult, but once created they escape the fireball without reinteraction, turning them into direct probes of the conditions under which they were created. The shape of their transverse momentum and invariant mass spectra has long been advertised as a direct probe of the extremely hot temperatures during the earliest stages of the expanding fireball. We here study these spectra at the next finer level of detail, by analyzing their anisotropies, especially their elliptic flow, in non-central collisions. Our goal is to use such measurements to illuminate with better resolution the early evolution of the fireball's spatial deformation through its imprint on the momentum anisotropies of the photons emitted during these early stages. Future studies will further complement the analysis presented here by directly measuring the space-time structure of the early collision fireball with two-photon correlations.

2 Spectra and elliptic flow

Both real and virtual photon (dilepton) momentum spectra can be written as

$$E dN/d^3p = \int [(\dots) \exp(-p \cdot u(x)/T(x))] d^4x, \quad (1)$$

where the quantity inside the square brackets indicates the thermal emission rates from the QGP or hadronic matter. The photon 4-momentum is parametrized by its rapidity Y , its transverse momentum $p_T = (p_x^2 + p_y^2)^{1/2}$, and its azimuthal emission angle ϕ as $p^\mu = (M_T \cosh Y, p_T \cos \phi, p_T \sin \phi, p_T \sinh Y)$. For real photons $M_T = p_T$; for dileptons $M_T = [M^2 + p_T^2]^{1/2}$ where M is the invariant mass of the virtual photon and lepton pair. The spectral shape is dominated by the Boltzmann factor describing a flow-boosted thermal distribution. Assuming boost-invariant longitudinal expansion and using standard proper time and space-time rapidity coordinates, it is given by

$$\frac{p \cdot u(x)}{T(x)} = \frac{\gamma_T(x)}{T(x)} \left[M_T \cosh(Y - \eta) - p_T v_T(x) \cos(\phi - \phi_v(x)) \right], \quad (2)$$

where v_T (with $\gamma_T = (1 - v_T^2)^{-1/2}$) is the magnitude and $\phi_v = \tan^{-1}(v_y/v_x)$ the azimuthal angle of the transverse flow velocity.

The azimuthal anisotropy (ϕ -dependence) of the spectrum is controlled by an interplay between the collective flow anisotropy and the geometric deformation of the temperature field $T(x, y, \tau)$ at non-zero impact parameter. In the present work both are given by a hydrodynamical calculation, using the

boost invariant hydrodynamic code AZHYDRO [5] with standard [5] initial conditions for Au+Au collisions at $\sqrt{s} = 200 A$ GeV. The only adjustment we make [6] is to extrapolate the initial entropy density from the usual initial time $\tau_0 = 0.6$ fm/ c to a 3 times smaller value $\tau_0 = 0.2$ fm/ c , assuming 1-dimensional boost-invariant expansion between these times, in order to account for at least a fraction of the pre-equilibrium photon production at very early times [7]. Its contribution to the photon spectrum is important at large p_T , and it will suppress its anisotropy there because very little transverse flow develops before 0.6 fm/ c .

We concentrate on photons and dileptons emitted at midrapidity $Y = 0$ so that the spectrum has only even azimuthal Fourier components v_n . The elliptic flow v_2 is computed as the angular average of $\cos(2\phi)$ with the spectrum (1) as weight function: $v_2 = \langle \cos(2\phi) \rangle$.

3 Thermal photons [6]

For the photon emission rate from the QGP phase we use the complete leading-order expression from Ref. [8], while the latest results in Ref. [9] are used for photon radiation from the hadron gas phase. The hadronic emission rate sums over a large number of hadronic rescattering channels. Figure 1 shows that these cluster into two different classes: at low p_T , photon production is dominated by *radiation* accompanying vector meson production from or decay into pions, whereas at large p_T collision induced *conversion* of vector mesons into photons dominates. Correspondingly the emitted photons trace the *pion*

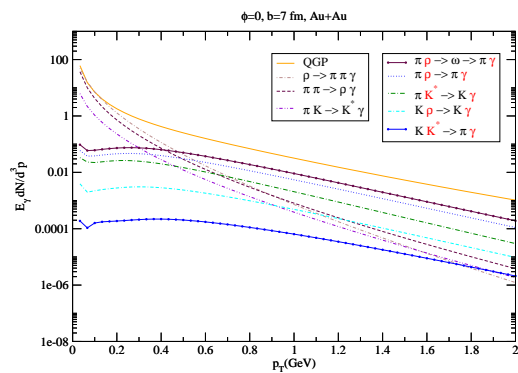


Fig. 1. Contributions to the photon p_T -spectrum at $\phi = 0$ from the QGP and from various hadronic rescattering channels during the late hadron gas phase.

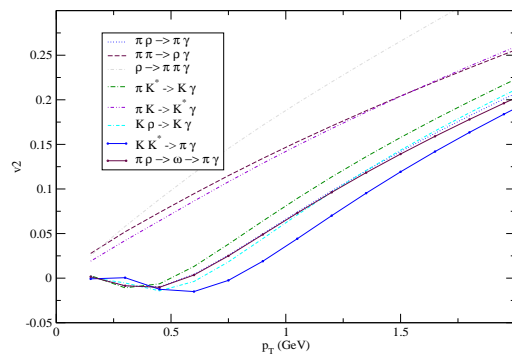


Fig. 2. Elliptic flows $v_2(p_T)$ associated with the individual hadronic photon contributions shown in Fig. 1 (Au+Au at $b = 7$ fm in both figures).

momentum distribution at low p_T and the *vector meson* momentum distribution at higher p_T . The latter is flattened by the effects of radial collective flow on the heavy vector mesons, exhibiting, in fact, a weak “blast wave peak” around $p_T = 0.4 - 0.5$ GeV/ c . This also explains why in Figure 2 the photons from $\pi\pi \rightarrow \rho\gamma$ etc. scattering exhibit the standard almost linear rise of the

elliptic flow v_2 with p_T , well known from the pions themselves, whereas the vector meson conversion photons carry much less elliptic flow, even contributing negatively at low p_T below the “blast wave peak” in their p_T spectrum.

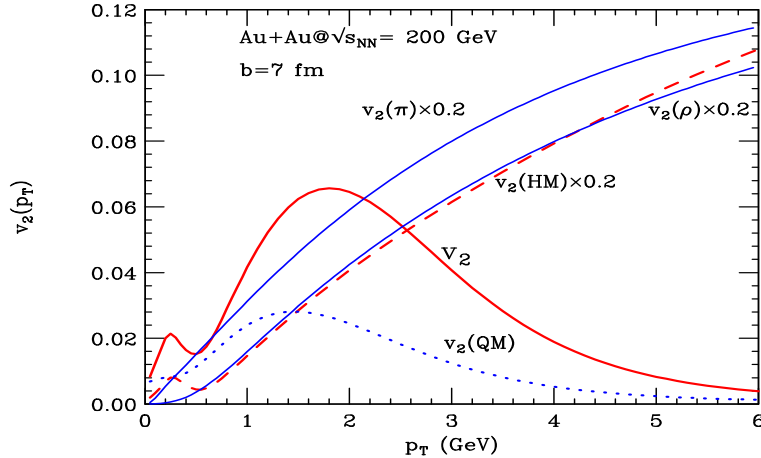


Fig. 3. Total photon elliptic flow $v_2(p_T)$, as well as hadronic and quark matter contributions for comparison. (Figure taken from [6].)

Figure 3 shows the total thermal photon elliptic flow (solid red line) and compares it with the elliptic flow of the early quark matter photons (dotted blue line) and of the late hadronic matter photons (dashed red line). Consistent with the spectra shown in Fig. 1, the hadron gas photons are seen to track the elliptic flow of pions at low p_T and that of ρ mesons at higher p_T (both shown by solid blue lines in Fig. 3 and exhibiting the almost linear rise of v_2 with p_T that is characteristic of hadrons in the hydrodynamic model [10]). The cross-over between these two patterns causes a distinctive peak-valley structure in v_2 around $p_T = 0.4 - 0.5 \text{ GeV}/c$. Since the hydrodynamic model is known to work quantitatively very well in this transverse momentum range [10], we expect this structure to be robust [11].

In contrast to the hadronic photons, the quark matter photons show an elliptic flow which decreases at high p_T . This reflects the fact that they track quark momenta, and that quark flow is small at early times when the high- p_T photons are emitted. As one goes down in p_T one probes later emission times and sees an increasing v_2 of the quark matter photons, reflecting the buildup of elliptic flow in the quark fluid. The behavior of the total photon elliptic flow, finally, can be understood by realizing that hadronic photons dominate the total photon spectrum only at low p_T while quark matter radiation begins to take over around $p_T \simeq 0.4 \text{ GeV}/c$, completely outshining the hadron gas for $p_T > 1 - 2 \text{ GeV}/c$. This cuts off the linear rise of the hadronic photon v_2 , and the total photon elliptic flow at high transverse momenta thus reflects the small elliptic flow during the very early collision stages.

One should remember, however, that ideal fluid dynamics gradually breaks down at higher p_T . Data suggest [12] that near the hadronization point quark

elliptic flow begins to be seriously affected by viscous effects for $p_T > 1 \text{ GeV}/c$, and this threshold may be even lower at earlier times when the longitudinal expansion rate is higher and shear viscous effects are larger. For $p_T > 1 \text{ GeV}/c$ our hydrodynamic prediction of photon elliptic flow must thus be regarded as an upper limit, and its already small values at large p_T will be further reduced by viscous corrections and prompt photon contributions [13,14].

4 Thermal dileptons [15]

With dileptons (virtual photons) we can probe the elliptic flow as a function of an additional variable, their invariant mass $M = M_{\ell\bar{\ell}} = M_{\gamma^*}$:

$$v_2(M, p_T; b) = \frac{\int d\phi \cos(2\phi) \frac{dN_{\ell\bar{\ell}}(b)}{dM^2 dY p_T dp_T d\phi}}{\int d\phi \frac{dN_{\ell\bar{\ell}}(b)}{dM^2 dY p_T dp_T d\phi}}. \quad (3)$$

In Figures 4 and 5 we show p_T -spectra and elliptic flow of thermal dileptons with invariant mass $M = m_\phi$. We see in Fig. 4 that for this value of M the p_T -spectrum is completely dominated by virtual photon emission from the hadronic phase, all the way up to $p_T = 4 \text{ GeV}/c$. The elliptic flow of the

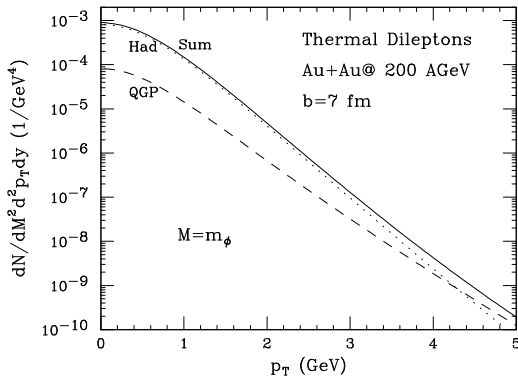


Fig. 4. The p_T -spectrum of thermal dileptons with mass $M = m_\phi$, showing the total spectrum as well as separate contributions from quark and hadronic matter.

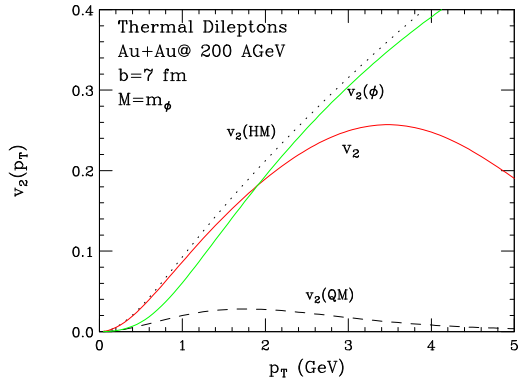


Fig. 5. $v_2(p_T)$ of thermal dileptons with $M = m_\phi$ (of quark and hadronic matter dileptons and of their sum), as well as of ϕ mesons emitted at thermal freeze-out.

dileptons emitted from the hadronic phase closely tracks that of ϕ -mesons at thermal freeze-out, as seen in Fig. 5. The elliptic flow of hadronic dileptons with $M = m_\phi$ (blue dotted line) is slightly larger than that ϕ mesons (green solid line) since radial flow (which suppresses v_2) continues to build up during the hadronic phase and the hadronic dileptons are on average emitted somewhat earlier than the ϕ mesons [16].

We have checked [15] that the calculated ϕ meson p_T -spectrum at thermal freeze-out agrees with the measured spectrum of ϕ mesons reconstructed from K^+K^- decays by the PHENIX Collaboration [17]. The elliptic flow of quark matter dileptons with $M = m_\phi$ (black dashed line in Fig. 5) is much smaller

and shows the same characteristic decrease at large p_T as the elliptic flow of thermal photons in Fig. 3, reflecting their early emission when the flow anisotropy of the quark fluid was still small. Due to the dominance of hadronic dileptons at this invariant mass, this decrease of v_2 at large p_T is seen in the overall elliptic flow only at very large $p_T > 4 \text{ GeV}/c$; below $p_T = 2 \text{ GeV}/c$, the total dilepton elliptic flow follows almost perfectly the hadronic v_2 .

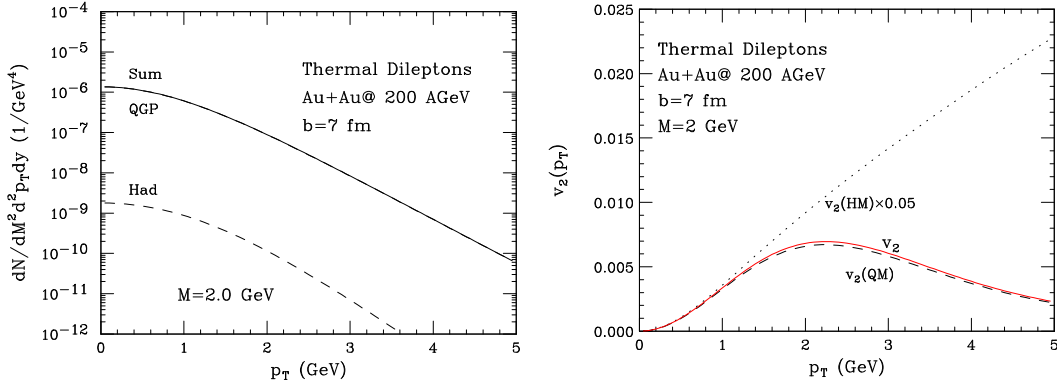


Fig. 6. Same as Fig 4, but for $M = 2 \text{ GeV}$. Fig. 7. Same as Fig 5, but for $M = 2 \text{ GeV}$.

Qualitatively the same pattern is observed for dileptons with invariant mass $M = m_\rho$ when compared with ρ mesons emitted at thermal freeze-out [15]. But things are different for dileptons with an invariant mass of $M = 2 \text{ GeV}$ (Figures 6 and 7). Now the QGP dileptons outshine those from the hadron gas for all p_T by three orders of magnitude or more. While the elliptic flow of the hadronic dileptons still shows the hydrodynamic almost linear rise with p_T (dotted line in Fig. 7), they are completely buried underneath the quark matter dileptons, and the total thermal dilepton spectrum at $M = 2 \text{ GeV}$ thus exhibits clearly the rise and fall of the elliptic flow with increasing p_T that is characteristic of emission from the early QGP phase.

The story is further clarified by studying the invariant mass dependence of the p_T -integrated elliptic spectrum (the “dilepton mass spectrum”, Figure 8) and of the corresponding p_T -integrated elliptic flow $v_2(M)$ (Figure 9). We note that these spectra are preliminary and do not properly account for the ω meson; complete mass spectra of the dilepton elliptic flow which include the ω contribution as well as dileptons from vector meson decays after thermal freeze-out will be presented in [15]. Figure 8 shows that near the vector mesons peaks (ρ , ω , ϕ), dilepton emission from the late hadronic stage dominates by at least an order of magnitude over QGP radiation. Correspondingly, the total dilepton elliptic flow approaches in these mass regions the value of the hadronic matter dileptons (dotted line in Fig. 9). If one adds the post-freeze-out vector meson decays, the total elliptic flow around $M = m_\omega$ and $M = m_\phi$ even approaches the elliptic flow of the corresponding hadrons, ω and ϕ , emitted at kinetic freeze-out. This last observation is explained by the relatively long lifetimes of the ω and ϕ mesons (23 and 45 fm/c, respectively), which signifi-

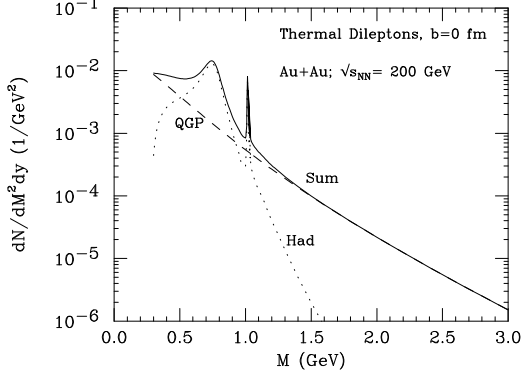


Fig. 8. QGP and hadron gas contributions to the dilepton invariant mass spectrum for 200 A GeV Au+Au collisions at $b=7$ fm. The solid line is the total dilepton mass spectrum.

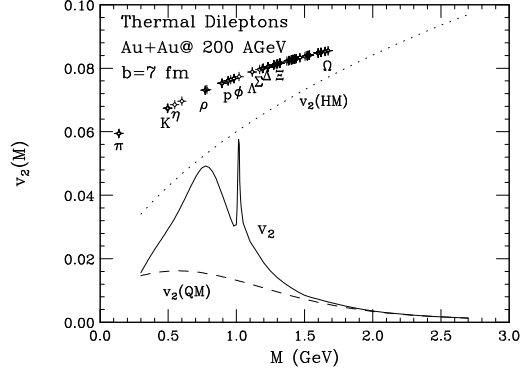


Fig. 9. The invariant mass dependence of the total p_T -integrated dilepton elliptic flow, as well as that of its hadron and quark matter contributions. Shown for comparison are also the p_T -integrated elliptic flows for a number of hadrons emitted at thermal freeze-out.

cantly exceeds the duration of the hadron gas phase (~ 7 fm/ c) such that on the resonance peaks dilepton emission from the hadron phase is overwhelmed by post-freeze-out dilepton decays of these resonances.

Note that the elliptic flow of the hadronic dileptons (dotted line in Fig. 9) remains significantly below that of the hadrons emitted at thermal freeze-out at $T_{\text{dec}} = 130$ MeV (crossed circles in Fig. 9). In view of the similarity of the p_T -dependences of their elliptic flows (see, e.g., the blue dotted and solid green lines in Fig. 5 this looks surprising. The puzzle is resolved by noting that, at a fixed invariant mass, the hadronic dilepton p_T -spectrum is steeper than the thermal freeze-out hadron spectrum for a hadron with the same mass [15]. The difference is likely due to additional radial flow built up between the average time of hadronic photon emission and final hadron freeze-out.

5 Conclusions

Elliptic flow of thermal photons and dileptons was shown to be a versatile and potentially powerful probe of the fireball dynamics at RHIC and LHC, complementary to the already well-studied flow anisotropies in the hadronic sector. Contrary to hadron elliptic flow, which in a hydrodynamic picture rises monotonically with increasing p_T and in real life, due to viscous effects, saturates at high p_T , photon and dilepton elliptic flow decrease to zero at large p_T and large dilepton mass, reflecting direct emission from the early QGP at a stage when flow anisotropies have not yet had time to grow strong. $v_2^\gamma(p_T)$ and $v_2^{\ell\bar{\ell}}(M)$ exhibit rich structures which reflect the interplay of different emission processes, opening a window on detailed and differential information from a variety of different stages of the fireball expansion. The elliptic flow of photons and dileptons emitted from the late hadronic stage was seen to track the

v_2 of the emitting hadrons, which suggests the possibility of subtracting the hadronic photon contributions from the total (virtual) photon signal in order to isolate and study in greater detail the elliptic flow of early QGP photons.

Obviously, the measurements will be difficult and the theoretical treatment can use further refinement, but this first glimpse suggests that photon and dilepton elliptic flow have the potential of turning into profitable gold mines.

References

- [1] U. Heinz and P. F. Kolb, Nucl. Phys. A **702**, 269 (2002).
- [2] P. Huovinen, Nucl. Phys. A **761**, 296 (2005).
- [3] T. Hirano, U. Heinz, D. Kharzeev, R. Lacey and Y. Nara, Phys. Lett. B **636**, 299 (2006).
- [4] T. Lappi and R. Venugopalan, arXiv:nucl-th/0609021.
- [5] The code can be downloaded from URL <http://nt3.phys.columbia.edu/people/molnard/OSCAR/>. See also P. F. Kolb, J. Sollfrank and U. Heinz, Phys. Rev. C **62**, 054909 (2000), and P. F. Kolb and R. Rapp, Phys. Rev. C **67**, 044903 (2003).
- [6] R. Chatterjee, E. S. Frodermann, U. Heinz and D. K. Srivastava, Phys. Rev. Lett. **96**, 202302 (2006).
- [7] S. A. Bass, B. Müller and D. K. Srivastava, Phys. Rev. Lett. **93**, 162301 (2004).
- [8] P. Arnold, G. D. Moore, and L. G. Yaffe, JHEP **0112**, 009 (2001).
- [9] S. Turbide, R. Rapp, and C. Gale, Phys. Rev. C **69**, 014903 (2004).
- [10] P. F. Kolb and U. Heinz, in *Quark-Gluon Plasma 3*, edited by R.C. Hwa and X.-N. Wang (World Scientific, Singapore, 2004), p. 634 [nucl-th/0305084].
- [11] Some details may still change when hadron chemical freeze-out directly after hadronization near $T_c = 170$ MeV is properly taken into account, by assigning all hadrons appropriate T -dependent chemical potentials (see discussion in [5]) and folding these also into the photon emission rates. This was not done in [6].
- [12] U. Heinz, AIP Conf. Proc. **739**, 163 (2005).
- [13] R. J. Fries, B. Müller and D. K. Srivastava, Phys. Rev. Lett. **90**, 132301 (2003), and Phys. Rev. C **72**, 041902(R) (2005).
- [14] S. Turbide, C. Gale, and R. J. Fries, Phys. Rev. Lett. **96**, 032303 (2006).
- [15] R. Chatterjee, C. Gale, U. Heinz, and D.K. Srivastava, in preparation.
- [16] A recent calculation by Hirano *et al.* [18], using a hybrid hydro+cascade approach where the evolution after hadronization is described by a realistic hadron cascade, predicts that the ϕ mesons have larger elliptic flow $v_2(p_T)$ than shown in Fig. 5, similar to the blue dotted line in Fig. 5 describing the hadronic dileptons. This is due to viscous effects in the hadronic phase which do not allow the ϕ mesons to pick up quite as much radial flow as predicted by the ideal fluid dynamical simulation presented here.
- [17] S. S. Adler *et al.*, [PHENIX Collaboration], Phys. Rev. C **72**, 014903 (2005).
- [18] T. Hirano, U. Heinz, D. Kharzeev, R. Lacey, and Y. Nara, in preparation.